J. Fluid Mech. (1977), *vol.* 79, *part* 2, *pp.* 257–272
Printed in Great Britain

Experimental determination of the main features of the viscous flow in the wake of a circular cylinder in uniform translation. Part 2. Unsteady flow

By MADELEINE COUTANCEAU AND ROGER BOUARD

Laboratoire de Mécanique des Fluides, Université de Poitiers, France

(Received 24 May 1976)

The plane flow induced by the impulsive start of a circular cylinder previously at rest in a still fluid is investigated experimentally by a visualization technique. The details of the flow field at the different stages of its establishment are pointed out, and the effect of the wall upon the evolution of the flow in time is examined. Photographs of the flow patterns are presented. This study corresponds to that range of Reynolds numbers for which a closed wake exists and adheres stably to the cylinder.

1. Introduction

Using the apparatus and experimental technique described in part 1 of this paper, we have visualized, at different stages of its establishment, the flow produced when a circular cylinder, previously at rest in a still fluid, is impulsively set in motion at time $t = 0$ with a constant speed V_0 in a direction perpendicular to its generating lines. For this purpose, photographs were taken at different values of the Reynolds number Re and at different dimensionless times t^* after the start of the motion, where t^* is the ratio between the true time t and t_0, the time taken by the cylinder to cover a distance equal to its diameter D ($t^* = t/t_0$ with $t_0 = D/V_0$).

The range of Reynolds numbers (based on the cylinder diameter) that we have investigated corresponds approximately to the case where a stable closed attached wake exists downstream of the cylinder. Our experimental technique refers the fluid motion to axes moving with the cylinder, and we examine the influence of the wall by varying the ratio λ between the cylinder and tank diameters.

We shall compare our results with numerical and experimental data found in the literature. Theoretical investigations of the problem have, in most cases, obtained the features of the steady flow by a time-limit process (Payne 1958; Hirota & Miyakoda 1965; Kawaguti & Jain 1966; Ingham 1968; Jain & Rao 1969; Son & Hanratty 1969; Thoman & Szewczyk 1969; Collins & Dennis 1973; Wu & Thompson 1973). The work of Wang (1967) and Panikker & Lavan (1975), who were interested only in the initial behaviour of the flow for, respectively, $Re = 100$ and $Re = 500$, has also to be considered. There are very few experimental data concerning this problem. Honji & Taneda (1969) and Taneda (1972)

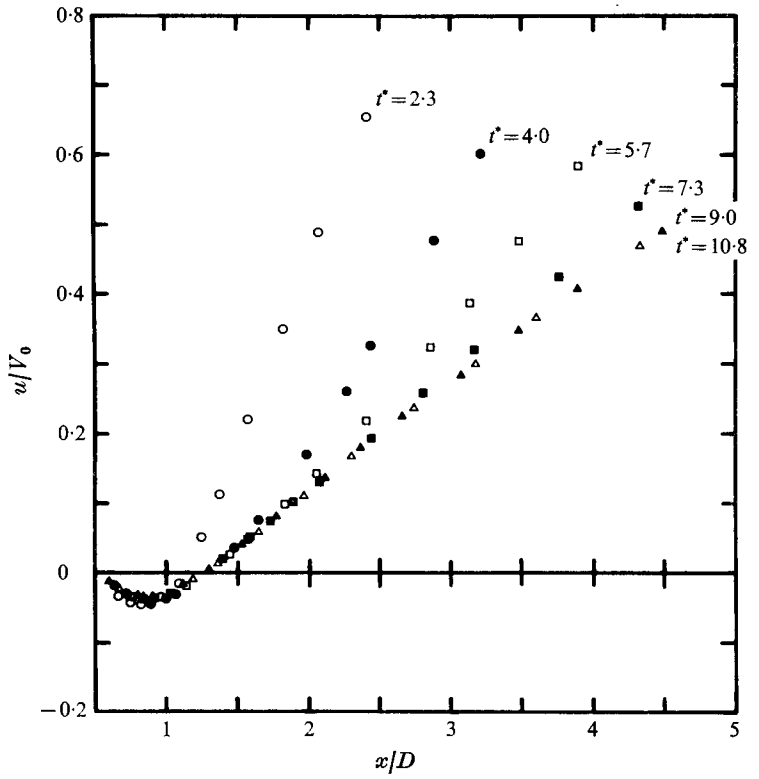

FIGURE 2. Velocity distribution on the flow axis behind a cylinder for different times t^* when $Re = 20$, $\lambda = 0{\cdot}07$.

study the evolution in time of the closed-wake length, but it seems that no measurement of the velocity distribution has been made. The motivation behind this research is, in particular, to provide detailed information in this field.

2. Flow pattern visualizations

The visualization photographs of figure 1 (plate 1) show the evolution of the flow in time when $Re = 42{\cdot}8$, $\lambda = 0{\cdot}12$ and $1{\cdot}1 \leqslant t^* \leqslant 6{\cdot}1$; these photographs have been made with a camera moving with the cylinder, the motion of the two being coupled by the apparatus. It is seen, in particular, that the wake spreads out as t^* increases. When the cylinder is set in motion the initial flow is irrotational everywhere; then the vorticity is progressively diffused from the cylinder wall and the flow separates from the body and forms standing eddies. The length, the separation angle and the width of this closed attached wake grows with time.

Such photographs, taken successively at regularly increasing times following the start of the cylinder, allow us to determine the evolution in time of the velocity field and of the various typical flow parameters, especially those concerning the closed wake.

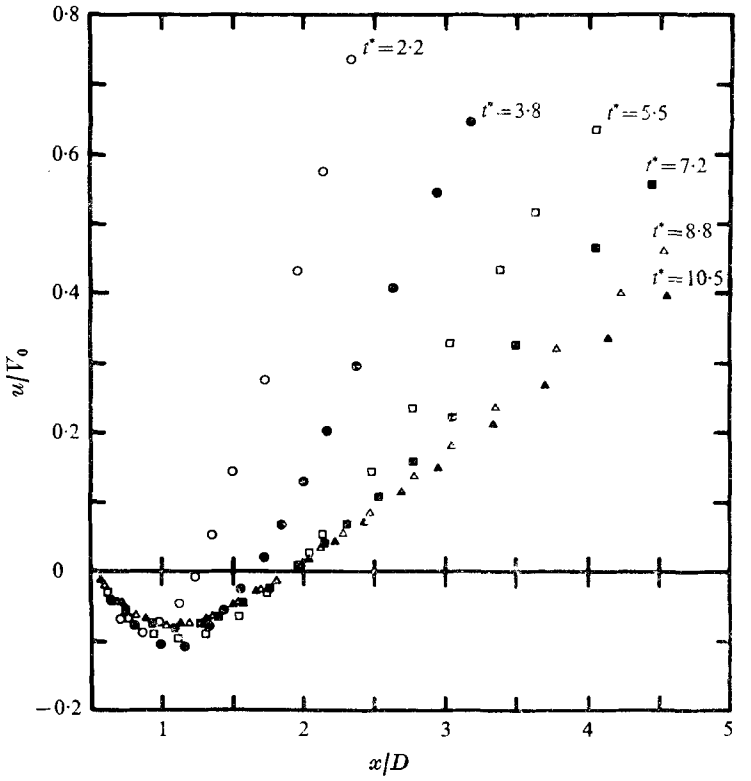

FIGURE 3. Velocity distribution on the flow axis behind a cylinder for different times t^* when $Re = 31·2$, $\lambda = 0·07$.

3. Evolution in time of the velocity distribution on the flow rear axis

Using methods similar to those described in the first part of this paper, we have measured the velocity distribution on the flow axis downstream of the cylinder for different values of each of the parameters governing the phenomenon: the Reynolds number Re, the diameter ratio λ and the time t^* measured from the impulsive start of the cylinder.

As an example, we give the evolution in time of the axial velocity distribution for $\lambda = 0·07$ and different Re values: $Re = 20$, figure 2; $Re = 31·2$, figure 3; $Re = 40$, figure 4. Analogous curves have been obtained when $\lambda = 0·024$ and $\lambda = 0·12$ and also for other Reynolds numbers. On these curves, the presence of the closed wake is revealed by the existence of negative velocities on part of the axis: in this wake, near the axis, the flow direction is opposite to the general one. The closed-wake length appears clearly: it is measured by the axial distance between the zero-velocity point and the rear stagnation point corresponding to the origin of the curves.

The analysis of the curves allows us to point out properties which, for the most part, do not seem to be mentioned in the literature:

(i) for a given Reynolds number and a given diameter ratio, the velocity curves evolve in time towards the limiting curve corresponding to the established

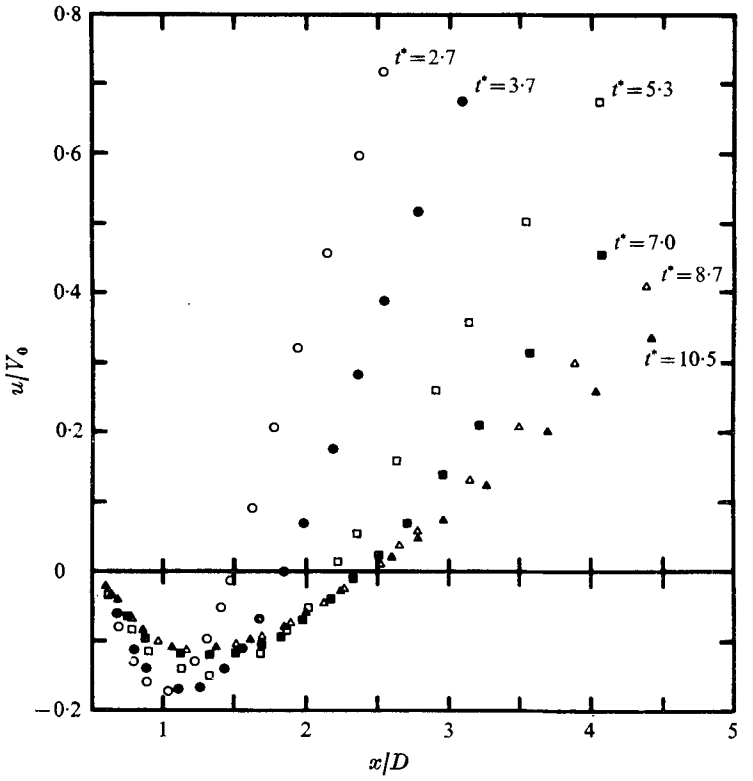

FIGURE 4. Velocity distribution on the flow axis behind a cylinder for different times t^* when $Re = 40$, $\lambda = 0{\cdot}07$.

regime,† the smaller the Reynolds number and the greater the ratio λ the more rapid the evolution;

(ii) when the closed-wake length is stabilized at its limiting value, the velocities still continue to evolve sensibly, during a certain period of time, within the standing eddies as well as outside this region;

(iii) the velocities are established more quickly inside the closed wake than outside, being, in general, established more and more slowly as one goes further away from the cylinder;

(iv) in the closed wake, during the flow establishment, the velocity reaches, at any given moment, a certain maximum value at a point on the flow axis. At a certain stage in the wake evolution, this velocity $U_{\max}$ goes through a maximum.

4. Evolution in time of the maximum velocity $U_{\max}$

In figure 5 we have represented graphically the variation of the maximum velocity $U_{\max}$ against the time t^* for $\lambda = 0{\cdot}07$ and $0{\cdot}12$ and for different Re values.

† We call 'established regime' the regime for which the evolution in time of the flow features, in the explored domain, is sufficiently faint not to be perceived by our measurement techniques.

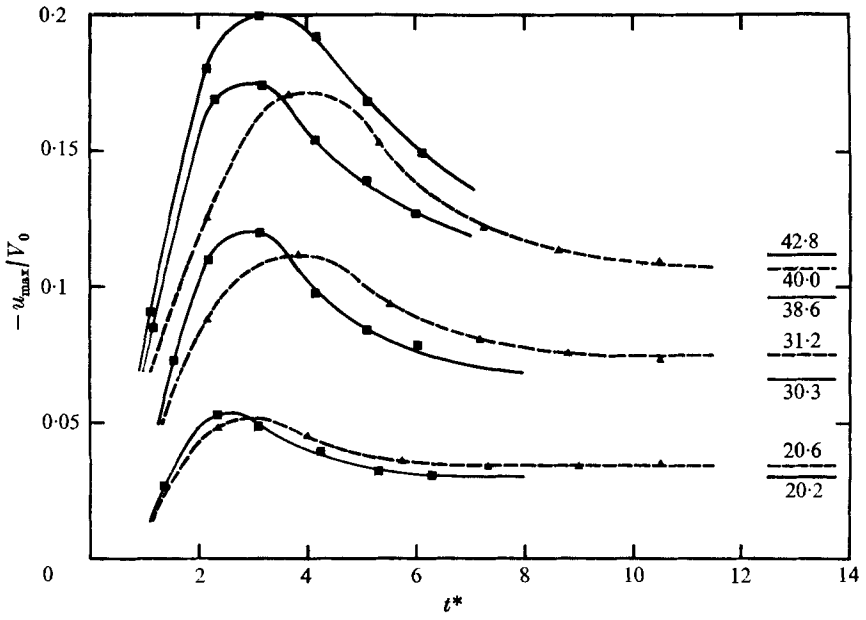

FIGURE 5. Evolution with time t^* of the maximum velocity on the flow axis within the cylinder wake for different values of Re and λ: ■, $\lambda = 0{\cdot}12$; ▲, $\lambda = 0{\cdot}07$.

The values for the established flow are added as limiting curves. The existence of the maximum just mentioned is clearly seen on these curves. It is seen that, for a given λ, the smaller the Reynolds number the sooner the corresponding 'peak' appears. This time deviation is, however, relatively small within the range of Reynolds numbers studied but it increases when λ decreases.

We remark also that the 'peak' occurs at a time t_p^* which becomes smaller as λ increases, i.e. as the wall comes nearer, especially as Re becomes higher.† Finally, it appears that for any given Reynolds number the height of the peak increases with λ, particularly at the higher values of Re, while for a given λ (i.e. for a given wall effect) the height of the peak increases with Reynolds number. The variation with Re is clearly stronger than the variation with λ.

Up to the present, this rather remarkable phenomenon of the existence of a peak does not seem to have been pointed out, either by theoretical investigators or by experimenters; however, the work of Honji (1975) suggests a similar effect at higher Reynolds numbers for starting flow down a step.

5. Evolution in time of the closed-wake geometrical parameters

The particular fineness of our visualization technique allows us to measure the main geometrical parameters of the closed wake with good accuracy, even during the first stages of its evolution. So that we can compare our present results

† Our curves do not correspond to exactly the same Re value for understandable experimental reasons, but taking into account the faint variation of t_p^* between the two Re values relative to each of the pair of curves, the phenomenon is unquestionable; furthermore it is confirmed by the curve drawn for $\lambda = 0{\cdot}12$ and $Re = 42{\cdot}8$.

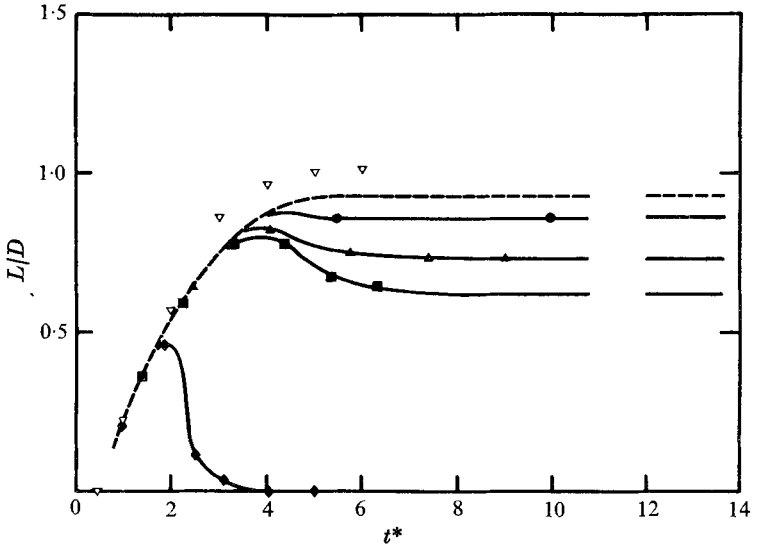

FIGURE 6. Evolution with time t^* of the cylinder closed-wake length for $Re \simeq 20$ and for different λ values: ◆, $\lambda = 0{\cdot}18$, $Re = 19{\cdot}7$; ■, $\lambda = 0{\cdot}12$, $Re \simeq 20{\cdot}4$; ▲, $\lambda = 0{\cdot}07$, $Re = 19{\cdot}9$; ●, $\lambda = 0{\cdot}024$, $Re = 20$; — —, $\lambda = 0$, $Re = 20$. Comparison with theoretical data: ▽, $Re = 20$, Kawaguti & Jain (1966).

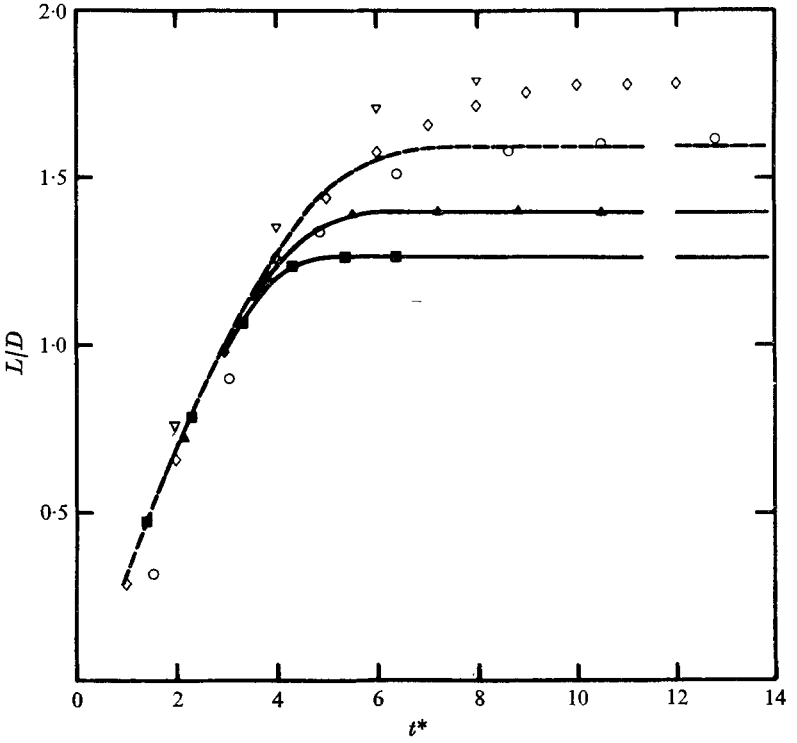

FIGURE 7. Evolution with time t^* of the cylinder closed-wake length for $Re \simeq 31$ and different λ values: ■, $\lambda = 0{\cdot}12$, $Re = 31{\cdot}5$; ▲, $\lambda = 0{\cdot}07$, $Re = 31{\cdot}2$; – – –, $\lambda = 0$, $Re = 31$. Comparison with theoretical data: ▽, $Re = 30$, Kawaguti & Jain (1966); ◇, $Re = 30$, Thoman & Szewczyk (1969). Comparison with experimental measurements: ○, $Re = 31{\cdot}2$, Honji & Taneda (1969).

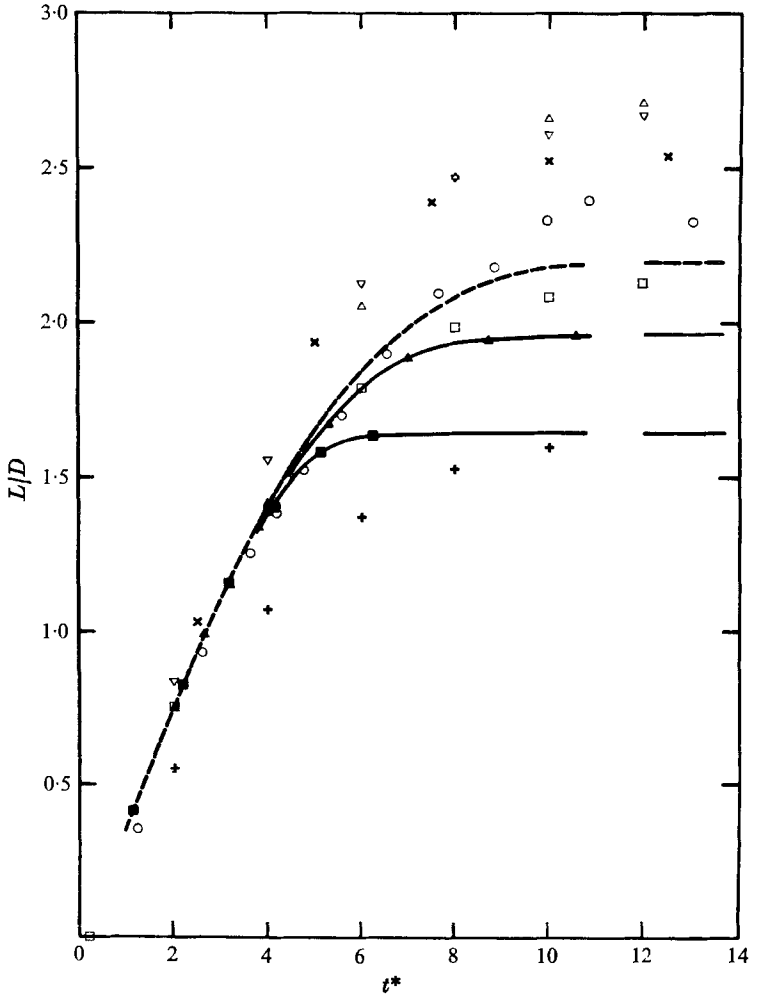

FIGURE 8. Evolution with time t^* of the cylinder closed-wake length for $Re \simeq 40$ and different λ values: ■, $\lambda = 0{\cdot}12$, $Re = 38{\cdot}6$; ▲, $\lambda = 0{\cdot}07$, $Re = 41$; ——, $\lambda = 0$, $Re = 40$. Comparison with theoretical data for $Re = 40$: ▽, Kawaguti & Jain (1966); +, Ingham (1968); △, Jain & Rao (1969); ×, Son & Hanratty (1969); □, Collins & Dennis (1973). Comparison with experimental measurements: ○, $Re = 40$, Honji & Taneda (1969).

with those obtained in part 1 of this paper, we now give the length of the wake, the position of the vortex cores, the separation angle and the shape of the closed wake.

Wake length L

The evolution in time of the closed-wake length L has been studied, on the one hand, at constant Re for different λ values, and, on the other hand, at constant λ for different Re values, in order to isolate the respective effects of each of these parameters.

Influence of the wall upon the variation of L in time. In figures 6–8 the variation of the length L in time for different values of λ is shown when $Re \simeq 20$, 31 and 40,

respectively. The important, and sometimes remarkable, effect of the wall upon the evolution in time of L is clearly shown by these curves. Extrapolating the results down to $\lambda = 0$, the curves relative to the unbounded flow have been deduced. The wake lengths corresponding to the established regime, as given in part 1, are indicated as limiting values. We have also compared, in these figures, the theoretical results obtained by different authors using numerical methods, and the experimental data given by Honji & Taneda (1969) and Taneda (1972).

The analysis of our curves shows the following at a given Re value.

(i) For the wake length, the more important the wall effect the shorter the establishment period; we have made a similar remark for the velocities previously.

(ii) The evolution in time of the wake length is independent of the ratio λ at the beginning of the motion: during this initial period, the wall has no sensible effect and the length is the same as it is in the case of an unbounded flow.

(iii) Below a certain Reynolds number, the evolution has an interesting character: the wake length passes through a maximum value, at which time the closed wake is more spread out than it is when established. This phenomenon, which appears clearly on the curves of figure 6, when $Re \simeq 20$, is probably caused by a wall effect because the greater the value of λ the more significant is the phenomenon. It is particularly pronounced and even spectacular in the case $\lambda = 0{\cdot}18$ and $Re \simeq 20$, where we see that the standing eddies appear, increase for a certain time, then decrease so much that they disappear completely, so that in the established regime these eddies no longer exist for these parameter values. This phenomenon can be considered as a consequence of the two remarks that we have made before: for small Reynolds numbers the wake-length establishment is more rapid and the wall effects do not occur sensibly at the beginning of the motion, so that, when these effects occur, they cause a regression of the closed wake which had developed as though there were no wall effect.

(iv) The greater the ratio λ the more quickly the wake length reaches its maximum.

Comparing now the results found in the literature, we find that, in a general way, during the initial period of the evolution, the results obtained by theoretical methods are close enough to those that we have deduced from our experiments, but they deviate more or less rapidly afterwards (Kawaguti & Jain 1966; Thoman & Szewczyk 1969; Son & Hanratty 1969; Jain & Rao 1969). From this point of view and for $Re = 40$, Collins & Dennis's results (1973) agree most with ours and those of Payne (1958), Ingham (1968), Wu & Thompson (1973) differ most.

From the analysis of the experimental results of Honji & Taneda (1969), it appears that the average evolution of the wake length is comparable with ours, but the dispersion of their points is rather marked, especially in the first part of the motion and for their smallest Reynolds number values. There, the standing eddies being very small, the measurements are difficult particularly as these authors determined the closed-wake length directly on the photographs. As we have mentioned before, our method using the velocity curves is certainly more accurate.

Influence of the Reynolds number upon the variation of L in time. The variation in time, for different Reynolds numbers of the length L, has been represented

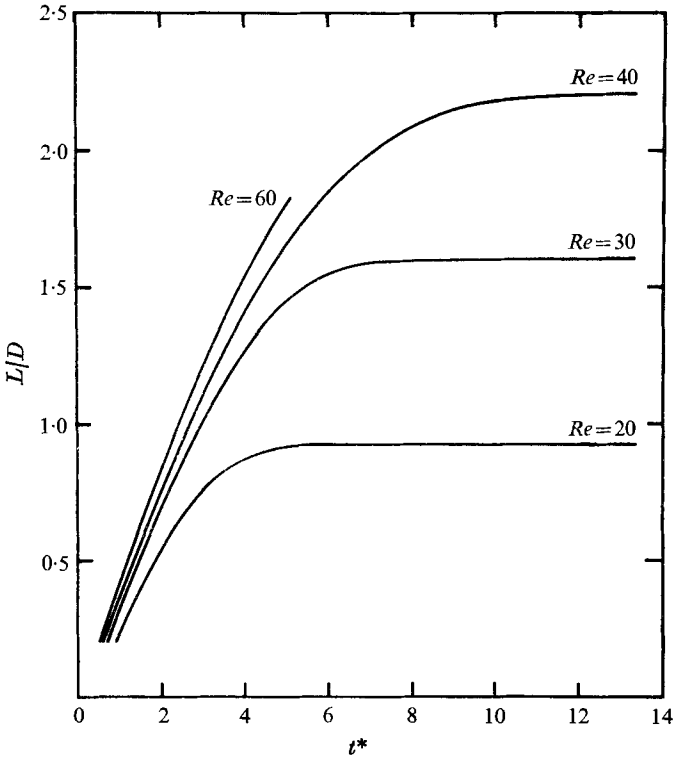

FIGURE 9. Evolution with time t^* of the cylinder closed-wake length for $\lambda = 0$.

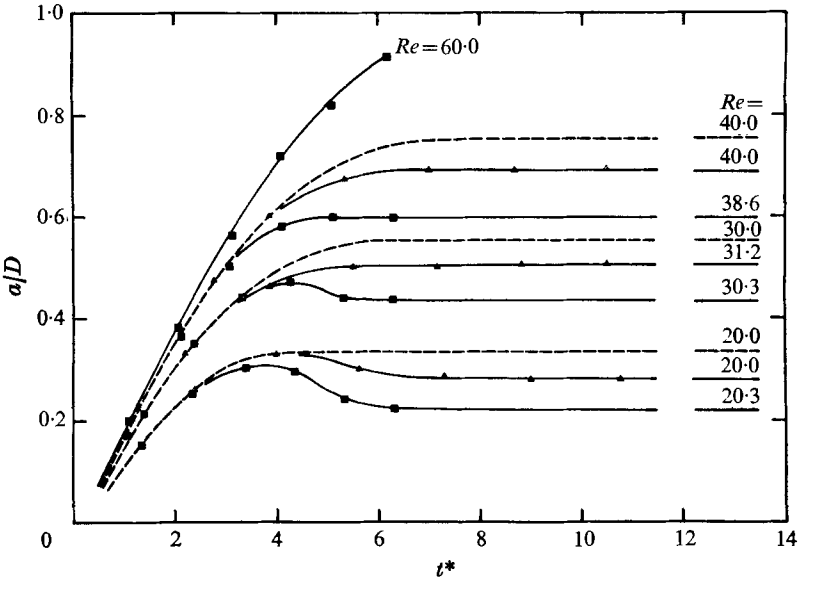

FIGURE 10. Evolution with time t^* of the cylinder closed-wake core abscissa for different values of Re and λ: ■, $\lambda = 0{\cdot}12$; ▲, $\lambda = 0{\cdot}07$; — —, $\lambda = 0$.

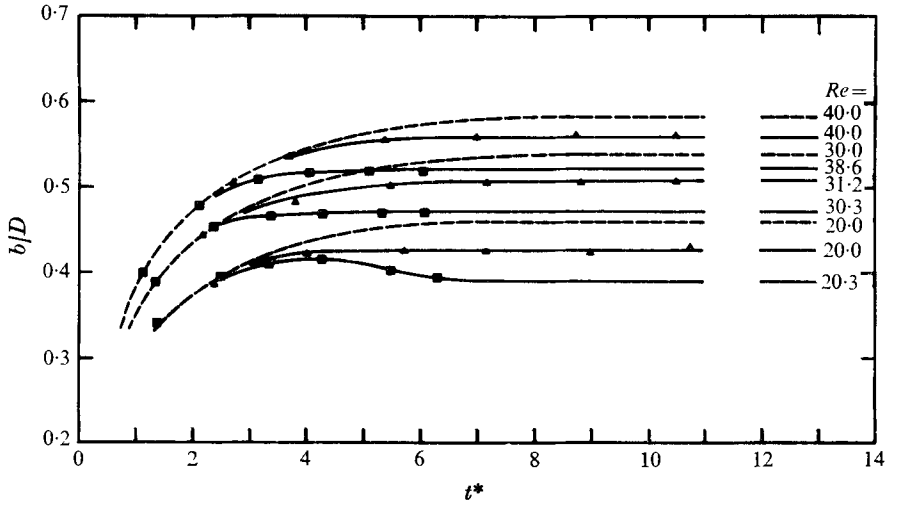

FIGURE 11. Evolution with time t^* of the cylinder closed-wake core ordinate for different values of Re and λ: ■, $\lambda = 0{\cdot}12$; ▲, $\lambda = 0{\cdot}07$; — —, $\lambda = 0$.

graphically in figure 9 for the case of infinite flow ($\lambda = 0$). We see that the closed-wake length is almost a linear function of time at the beginning of the establishment period. Then the curves tend towards their asymptotic value, doing so more quickly for small Re.

In contrast to what Honji & Taneda proposed for $31 < Re < 1500$, we find that the linear sections of the curves of L against t^* for different Reynolds numbers do not coincide. However, the greater the Reynolds number the smaller is the difference between the straight sections, and in the case $Re > 100$, which we have not investigated here, it is possible that the deviations become so faint that they are no longer measurable and that therefore the straight lines seem to be the same.

Evolution in time of the position of the vortex cores (a, b)

The position of the vortex cores is located by the distances a and b: a represents the distance between the line that joins the cores and the rear stagnation point, and b is the distance between the cores.

Influence of Re and λ *upon the evolution of* a. The variation of the distance a with the time t^* is presented in figure 10 for $\lambda = 0{\cdot}07$ and $0{\cdot}12$, and several values of Re. We find behaviour similar to that of the wake length L. In particular, when $Re \simeq 20$ the value of a is greater, for a time, than it is for the established regime. This behaviour is still measurable when $Re \simeq 30$ and $\lambda = 0{\cdot}12$, and, within experimental accuracy, is more pronounced than it is for the wake length.

On the other hand, from the curves of a against t^* for different values of λ but a constant Reynolds number, it appears that the curves are merged during the first phase of the motion, showing again that the wall effect is perceptible only after a certain lapse of time.

Influence of Re and λ *upon the evolution of* b. We give in figure 11 the evolution

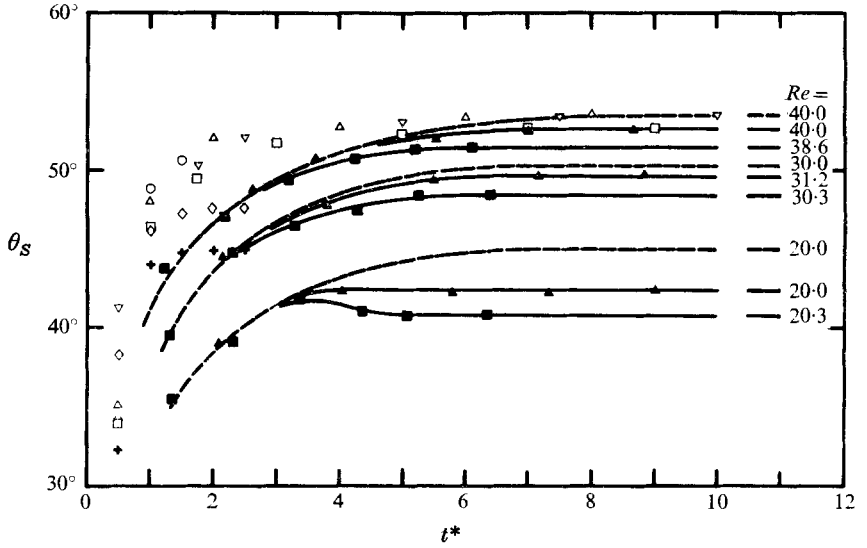

FIGURE 12. Evolution with time t^* of the cylinder closed-wake separation angle for different λ values: ■, $\lambda = 0{\cdot}12$; ▲, $\lambda = 0{\cdot}07$; — —, $\lambda = 0$. Comparison with theoretical results: △, Kawaguti & Jain (1966); □, Jain & Rao (1969); ▽, Son & Hanratty (1969); ◇, Thoman & Szewczyk (1969); ○, Collins & Dennis (1973), $Re = 40$; +, Thoman & Szewczyk (1969), $Re = 30$.

of the distance b that characterizes the cross-section of the closed wake. Close to the start of the motion, the distance b changes more rapidly than the corresponding wake longitudinal characteristics; afterwards, however, it is slower. On the whole, the establishment period is shorter than the period associated with a and L. For these parameters, we could not compare our results with other results; it seems that these characteristics have been neither calculated, nor measured.

Evolution in time of the separation angle

We have measured the separation angle θ_S corresponding to the separation of the main flow from the wall of the cylinder and we have studied its variation in time for the same Reynolds numbers and the same diameter ratios λ as those selected before. We give in figure 12 the corresponding evolutions, together with the theoretical results of Kawaguti & Jain, Son & Hanratty, Thoman & Szewzyk, Jain & Rao and Collins & Dennis. No experimental result seems to have been published for this feature.

The accurate determination of θ_S is difficult especially during the initial stage of the flow development when, on the one hand, the values are very small and, on the other, as is shown in figure 12, the variations are abrupt; cumulative errors result in the length and time measurements.

For very small times, most theoretical results seem to fit well with the prolongation of the curve that we have deduced from our experiments by extrapolation down to $\lambda = 0$. For $1 < t^* < 5$ they differ sensibly whereas for $t^* > 5$ the results of Kawaguti & Jain and Son & Hanratty again agree satisfactorily.

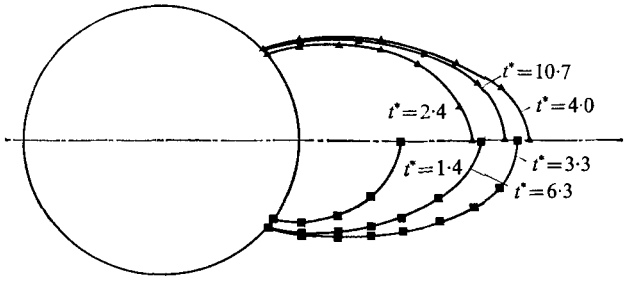

FIGURE 13. Evolution with time t^* of the cylinder closed-wake shape for different λ values: ■, $\lambda = 0{\cdot}12$, $Re = 20{\cdot}3$; ▲, $\lambda = 0{\cdot}07$; $Re = 20$.

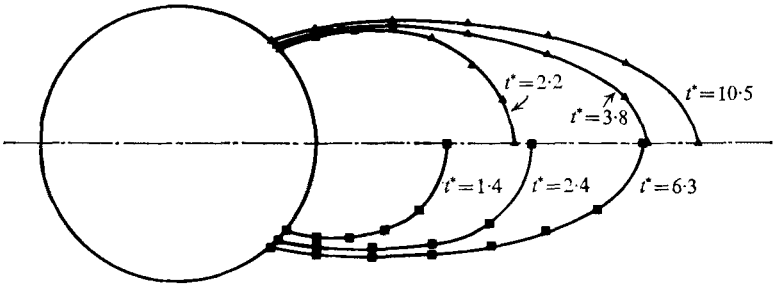

FIGURE 14. Evolution with time t^* of the cylinder closed-wake shape for different λ values: ■, $\lambda = 0{\cdot}12$, $Re = 30{\cdot}3$; ▲, $\lambda = 0{\cdot}07$, $Re = 31{\cdot}2$.

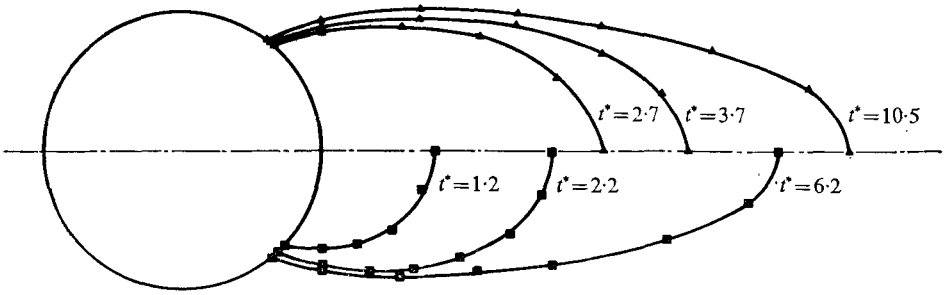

FIGURE 15. Evolution with time t^* of the cylinder closed-wake shape for different λ values: ■, $\lambda = 0{\cdot}12$, $Re = 38{\cdot}6$; ▲, $\lambda = 0{\cdot}07$, $Re = 40$.

Evolution in time of the attached-wake shape

The evolution of the outside boundary of the attached wake has been determined during the establishment period for $\lambda = 0{\cdot}07$ and $\lambda = 0{\cdot}12$. The corresponding graphic representations are given in figures 13–15, for Reynolds numbers of about 20, 31 and 40, respectively.

No comparisons are possible because, with the exception of Thoman & Szewczyk (and their figures are too small to allow us accurate readings), authors have given only the steady-state values that they obtained, their purpose being to calculate the features of the established flow.

	Re \ t^*		0·5	1	1·5	2	2·5	4	6	8	10	12
Kawaguti & Jain (1966)	20	L	0	0·23	0·42	0·57	0·69	0·97	1·01			
	30	L	0·09	0·35	0·57	0·76	0·90	1·36	1·71	1·79		
	40	L	0·12	0·40	0·62	0·85	1·01	1·56	2·13	2·48	2·51	2·515*
	40	θ_S	35·2°	48·1°	50·6°	51·7°	52·2°	52·8°	53·2°	53·4°	53·7°	53·7°*
Ingham (1968)	40	L	0·26	0·44	0·60	0·76	1·07	1·37	1·53	1·60		
Thoman & Szewczyk (1969)	30	L	0·10	0·28	0·48	0·66	0·82	1·25	1·57	1·71	1·77	1·79
	30	θ_S	32·5°	44·2°	44·8°	45·0°	45·0°					
	40	θ_S	39°	46·6°	47·4°	47·7°	47·8°					
Jain & Rao (1969)	40	L	0·13	0·32	0·51	0·71	0·92	1·44	2·03	2·48	2·64	2·65
		θ_S	33·9°	45·8°	49·2°	50·7°	51·3°	51·9°	52·4°	52·6°	52·7°	52·7°
Son & Hanratty (1969)	40	L	0·14	0·36	0·64	0·85	1·06	1·63	2·20	2·45	2·54	2·54
		θ_S	41°	49°	50·6°	51·5°	52°	52·7°	53·3°	53·5°	53·7°	53·7°
Collins & Dennis (1973)	40	L	0·09	0·33	0·58	0·78	0·97	1·42	1·81	2·00	2·11	2·16
		θ_S	33·8°	48·3°	50·3°							
Wu & Thompson (1973)	36	L			0·20	0·32	0·44	0·77	1·17	1·46	1·70	1·88

TABLE 1. Numerical values of the closed-wake parameters L and θ_S given by different authors for an indefinitely extended flow.

The boundaries that we have drawn for the highest values of t^* correspond, in practice, to the established flow (except in the case $\lambda = 0{\cdot}12$, $Re = 38{\cdot}6$), and therefore these figures show that the wake-shape variation is very strong in the initial stages, i.e. between $0 < t^* < t_L^*$, t_L^* being almost independent of λ. This stage of the motion corresponds, in fact, to the stage when the wall effect is negligible and the evolution of the features of the wake is quasi-linear.

It was noticed that, at the beginning of the establishment period, the evolution of θ_S and of the maximum closed-wake width was more rapid than the evolution of the length.

In the case $Re = 20$, the phenomenon that we have mentioned is particularly well pointed out: the closed wake is larger, at a given instant of the evolution, than it is when the flow is established.

List of the principal numerical data

In table 1 we have collected the values of the length L and of the separation angle θ_S, for a flow of indefinite extent, given in the literature either by means of curves† or by means of numerical values (these we have indicated by *). In table 2 we have recapitulated the values of L, θ_S, a and b deduced from our experiments when $Re \simeq 20$, 31, 40 and $\lambda = 0$, 0·07, 0·12 and $0 < t^* \leqslant 12$.

From the analysis of our results, it appears that the flow in the closed-wake regime can be considered as stabilized for the Reynolds numbers 20, 31, 40 when the times t^* are respectively equal to or greater than 9, 10, 12 for $\lambda = 0{\cdot}07$, and 10, 9, 10 for $\lambda = 0{\cdot}12$. As the evolution of velocities is slower than the evolution of the geometrical parameters of the wake, the times that we give are those for the establishment of the velocities.

† The values read on the curves of the cited authors may be lacking in precision because their diagrams are sometimes printed using a very small scale.

λ	Re \ t^*	...	1	2	3	4	5	6	8	10	12
0·12	20·4	L	0·22	0·54	0·75	0·80	0·72	0·65	0·62	0·62	0·62
	20·3	a	0·12	0·23	0·29	0·31	0·26	0·23	0·22	0·22	0·22
		b		0·37	0·40	0·42	0·41	0·40	0·39	0·39	0·39
		θ_s		38·4°	41·2°	41·4°	40·8°	40·7°	40·6°	40·6°	40·6°
0·07	19·9	L	0·22	0·54	0·75	0·83	0·78	0·75	0·74	0·73	0·73
	20	a	0·12	0·23	0·31	0·33	0·32	0·29	0·28	0·28	0·28
		b		0·37	0·41	0·42	0·43	0·43	0·43	0·43	0·43
		θ_s		38·4°	41·4°	42·3°	42·2°	42·2°	42·2°	42·2°	42·2°
0·024	20	L	0·22	0·54	0·75	0·87	0·87	0·87	0·87	0·87	0·87
0	20	L	0·22	0·54	0·75	0·88	0·93	0·93	0·93	0·93	0·93
		a	0·12	0·23	0·31	0·33	0·33	0·33	0·33	0·33	0·33
		b		0·37	0·41	0·44	0·45	0·46	0·46	0·46	0·46
		θ_s		38·4°	41·4°	43·1°	44·1°	44·7°	44·9°	44·9°	44·4°
0·12	31·5	L	0·32	0·70	1·00	1·21	1·25	1·26	1·26	1·26	1·26
	30·3	a	0·15	0·32	0·42	0·47	0·45	0·44	0·43	0·43	0·43
		b	0·35	0·43	0·46	0·47	0·47	0·47	0·47	0·47	0·47
		θ_s		43·5°	46°	47·4°	48·1°	48·2°	48·2°	48·2°	48·2°
0·07	31·2	L	0·32	0·70	1·03	1·24	1·36	1·39	1·39	1·39	1·39
		a	0·15	0·32	0·42	0·48	0·50	0·51	0·51	0·51	0·51
		b	0·35	0·43	0·47	0·49	0·50	0·51	0·51	0·51	0·51
		θ_s		43·5°	46·4°	48·1°	49·1°	49·4°	49·4°	49·4°	49·4°
0	31	L	0·32	0·70	1·03	1·28	1·47	1·56	1·59	1·59	1·59
	30	a	0·15	0·22	0·42	0·49	0·54	0·55	0·55	0·55	0·55
		b	0·35	0·43	0·48	0·50	0·52	0·53	0·54	0·54	0·54
		θ_s		43·5°	46·7°	48·5°	49·5°	50°	50·1°	50·1°	50·1°
0·12	38·6	L	0·36	0·74	1·11	1·38	1·57	1·63	1·64	1·64	1·64
		a	0·17	0·36	0·51	0·58	0·60	0·60	0·60	0·60	0·60
		b	0·38	0·47	0·51	0·52	0·52	0·52	0·52	0·52	0·52
		θ_s	41·2°	46·5°	49·1°	50·4°	51·1°	51·3°	51·3°	51·3°	51·3°
0·07	41	L	0·36	0·74	1·11	1·41	1·62	1·79	1·94	1·96	1·96
	40	a	0·17	0·36	0·51	0·61	0·66	0·69	0·69	0·69	0·69
		b	0·38	0·47	0·52	0·54	0·55	0·56	0·56	0·56	0·56
		θ_s	41·2°	46·5°	49·3°	51°	51·8°	52·3°	52·5°	52·5°	52·5°
0	40	L	0·36	0·74	1·11	1·41	1·65	1·85	2·05	2·18	2·19
		a	0·17	0·36	0·51	0·62	0·69	0·73	0·75	0·75	0·75
		b	0·38	0·47	0·52	0·55	0·56	0·58	0·59	0·59	0·59
		θ_s	41·2°	46·5°	49·3°	51°	52·1°	52·7°	53·1°	53·4°	53·4°

TABLE 2. Numerical values of the closed-wake geometrical parameters deduced from our experiments.

6. Conclusion

The study that we have presented here of the unsteady plane flow induced by the impulsive start of a cylinder previously at rest in a still viscous fluid allows us to point out some general properties concerning the evolution of the hydrodynamic field, especially in the closed wake:

(i) at the beginning of the motion, the transverse features evolve more quickly than the longitudinal features;

(ii) the closed-wake geometrical parameters are stabilized sooner than the velocity field, particularly on the flow axis, so that, when the theoreticians limit their investigation to the calculation of these geometrical parameters, the flow can appear to them as established when in fact it is not;

(iii) in general, a wall effect speeds up the establishment of the flow, although this is not always the case for the lower Reynolds numbers;

(iv) the greater the Reynolds number is the more rapid is the evolution in time at the beginning of the motion; the total establishment time, however, is greater.

Further, the systematic analysis of the wall effect has shown that the establishment period can be divided into two stages: a first stage when no perceptible wall effect exists and the flow develops as though indefinitely extended, and a second stage when the wall effect appears clearly and accelerates the evolution in time.

The fact that the wall effects are negligible at the beginning of the motion and that the establishment of the flow tends to be more rapid when the Reynolds numbers are small allows us to interpret the following phenomenon which has been pointed out experimentally: under certain conditions, the wake can be larger at certain moments of its evolution than it is in the established regime and it is even possible that it appears during the establishment period and disappears afterwards.

Finally, the precision of our measurements allows us to compare our results with those provided by theoretical investigations; the corresponding conclusions can serve as a verification and guidance to perfect the calculation techniques.

The authors are grateful to Prof. J. M. Bourot, Director of the Fluid Mechanics Laboratory of Poitiers, for supervising this research and they wish to thank J. R. Defaye for his help in translating this text into English and P. Falaise for contributing to the elaboration of efficient experimental techniques.

REFERENCES

COLLINS, W. M. & DENNIS, S. C. R. 1973 Flow past an impulsively started circular cylinder. *J. Fluid Mech.* **60**, 105.

HIROTA, I. & MIYAKODA, K. 1965 Numerical solution of Kármán vortex street behind a circular cylinder. *J. Met. Soc. Japan*, **43**, 30.

HONJI, H. 1975 The starting flow down a step. *J. Fluid Mech.* **69**, 229.

HONJI, H. & TANEDA, S. 1969 Unsteady flow past a circular cylinder. *J. Phys. Soc. Japan*, **27**, 1668.

INGHAM, D. B. 1968 Note on the numerical solution for unsteady viscous flow past a circular cylinder. *J. Fluid Mech.* **31**, 815.

JAIN, P. C. & RAO, K. S. 1969 Numerical solution of unsteady viscous incompressible fluid flow past a circular cylinder. *Phys. Fluids Suppl.* **12**, II 57.

KAWAGUTI, M. & JAIN, P. C. 1966 Numerical study of a viscous fluid flow past a circular cylinder. *J. Phys. Soc. Japan*, **21**, 10, 2055.

PANIKKER, P. K. G. & LAVAN, Z. 1975 Flow past impulsively started bodies using Green's functions. *J. Comp. Phys.* **18**, 46.

PAYNE, R. B. 1958 Calculations of unsteady viscous flow past a circular cylinder. *J. Fluid Mech.* **4**, 81.

SON, J. S. & HANRATTY, T. J. 1969 Numerical solution for the flow around a cylinder at Reynolds numbers of 40, 200 and 500. *J. Fluid Mech.* **35**, 369.

TANEDA, S. 1972 Visualization experiments on unsteady viscous flows around cylinders and plates. In *Récentes Recherches sur les Couches Limites Instationnaires*, vol. 2 (ed. E. A. Eichelbrenner), p. 1165. Quebec: Laval University Press.

THOMAN, D. C. & SZEWCZYK, A. A. 1969 Time-dependent viscous flow over a circular cylinder. *Phys. Fluids Suppl.* **12**, II 76.

WANG, C. Y. 1967 The flow past a circular cylinder which is started impulsively from rest. *J. Math. Phys.* **46**, 195.

WU, J. C. & THOMPSON, J. F. 1973 Numerical solution of time-dependent incompressible Navier–Stokes equations using an integro-differential formulation. *Computers & Fluids*, **1**, 197.

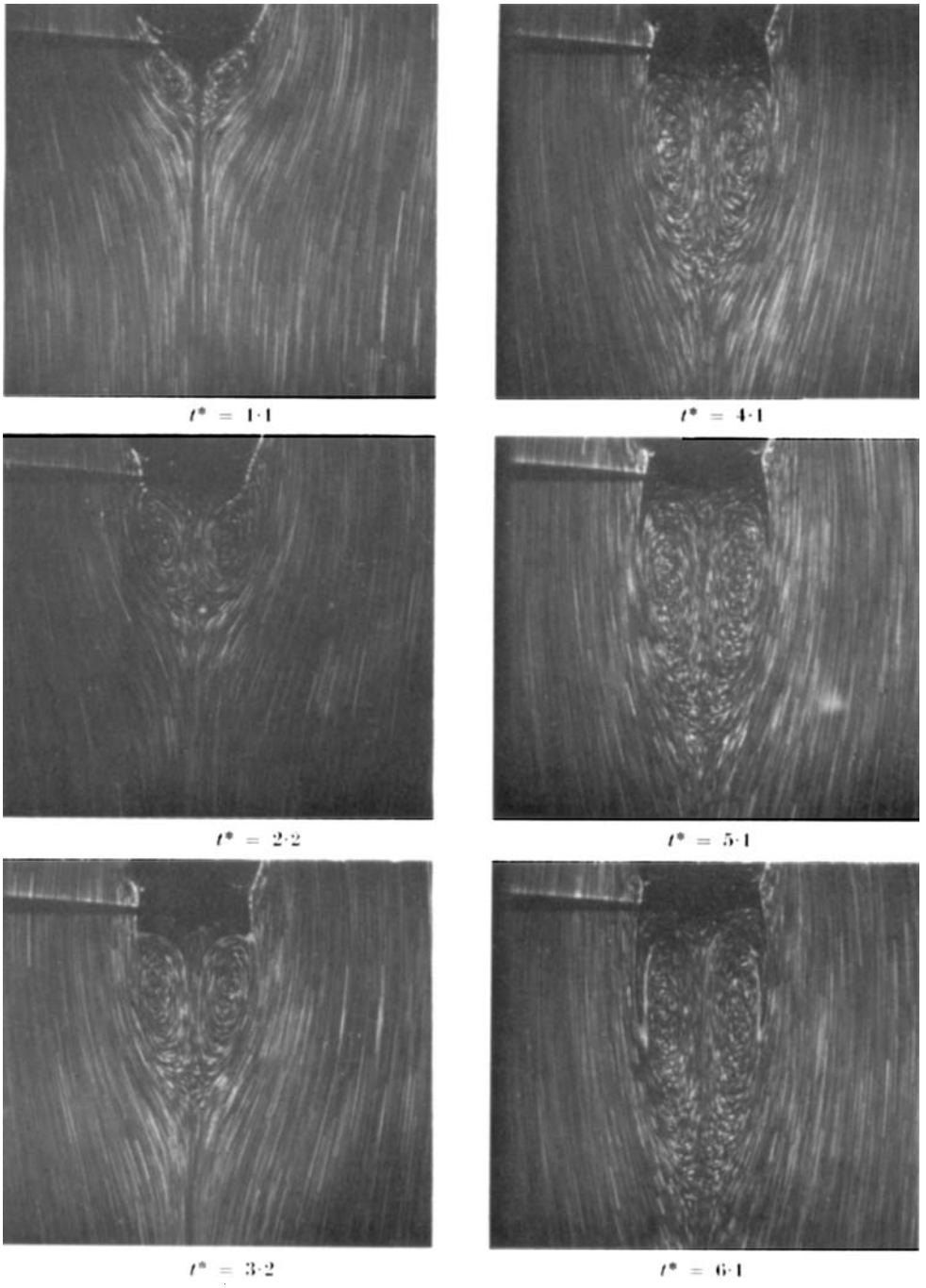

FIGURE 1. $Re = 42{\cdot}8$, $\lambda = 0{\cdot}12$.